

# NEXT-TO-LEADING ORDER $t\bar{t}$ PLUS JETS PHYSICS WITH HELAC-NLO

MALGORZATA WOREK<sup>a</sup>

*Fachbereich C Physik, Bergische Universität Wuppertal, D-42097 Wuppertal*

A report on the recent next-to-leading order QCD calculations to  $t\bar{t}b\bar{b}$  and  $t\bar{t}jj$  processes at the CERN Large Hadron Collider is presented. Results for integrated and differential cross sections are given. A significant reduction of the scale dependence is observed in both cases, which indicates that the perturbative expansion is well under control. The results are obtained in the framework of the HELAC-NLO system.

## 1 Introduction

For a light Higgs boson, with mass  $m_H \leq 135$  GeV the highest decay rate mode is  $H \rightarrow b\bar{b}$ . In the dominant Higgs boson production channel at the CERN Large Hadron Collider (LHC), i.e. in gluon fusion, this decay mode is not very highly considered because of its overwhelming QCD background. On the other hand, the associated production of a top quark pair with a Higgs boson includes more distinctive signature, which should provide a unique opportunity of independent direct measurement of Higgs boson Yukawa couplings to tops and bottoms. Whether or not it will also provide a discovery channel, depends very much on the ratio between this signal and the main QCD backgrounds. Early studies at ATLAS and CMS even suggested discovery potential, however, analyses with more realistic calculations of background processes, still only based on leading-order (LO) matrix elements, show problems if the latter are not very well controlled<sup>1,2</sup>. A careful and detailed examination of the backgrounds shows that the most relevant are the direct production of the final state  $t\bar{t}b\bar{b}$  (irreducible background) and the production of a top quark pair in association with two jets,  $t\bar{t}jj$  (reducible background). The latter needs to be taken into account due to the finite efficiency in identifying b-quarks in jets (b-tagging). The calculation of the next-to-leading-order (NLO) QCD corrections to both background processes can be regarded as a major step forward towards the observability of the  $t\bar{t}H \rightarrow t\bar{t}b\bar{b}$  signal at the LHC.

The calculations of the NLO QCD corrections to the  $pp \rightarrow t\bar{t}b\bar{b}$  process have been first presented last year<sup>3</sup> and subsequently confirmed by our group at the permille level<sup>4</sup>. Very recently, the NLO QCD corrections to  $pp \rightarrow t\bar{t}jj$  background process have been performed<sup>5</sup>. In this contribution, a brief report on these computations is given.

## 2 Details of the next-to-leading order calculation

The next-to-leading order results are obtained in the framework of HELAC-NLO based on the HELAC-PHEGAS leading-order event generator for all parton level processes<sup>6,7,8</sup>. The NLO

---

<sup>a</sup>Presented at the XLVth Rencontres de Moriond on QCD and High Energy Interactions, La Thuile (Aosta), Italy, March 13-20, 2010.

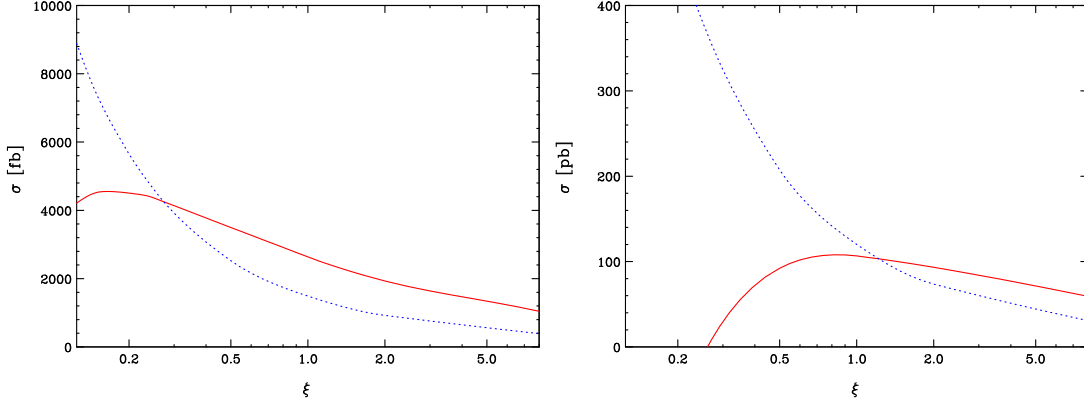


Figure 1: Scale dependence of the total cross section for  $pp \rightarrow t\bar{b}b\bar{b} + X$  (left panel) and for  $pp \rightarrow t\bar{t}jj + X$  (right panel) at the LHC with  $\mu_R = \mu_F = \xi \cdot \mu_0$  where  $\mu_0 = m_t = 172.6$  GeV. The blue dotted curve corresponds to the LO whereas the red solid to the NLO one.

system consists of: 1) CUTTOOLS<sup>9</sup>, for the OPP reduction of tensor integrals with a given numerator to a basis of scalar functions and for the rational parts<sup>10,11,12</sup>; 2) HELAC-1LOOP<sup>13</sup> for the evaluation of one loop amplitude, more specifically for the evaluation of the numerator functions for given loop momentum (fixed by CUTTOOLS); 3) ONELOOP<sup>13</sup>, a library of scalar functions, which provides the actual numerical values of the integrals. 4) HELAC-DIPOLES<sup>14</sup>, automatic implementation of Catani-Seymour dipole subtraction<sup>15</sup>, for the calculation of the real emission part.

Let us emphasize that all parts are calculated fully numerically in a completely automatic manner.

### 3 Numerical results

Proton-proton collisions at the LHC with a center of mass energy of  $\sqrt{s} = 14$  TeV are considered. The mass of the top quark is set to be  $m_t = 172.6$  GeV. We leave it on-shell with unrestricted kinematics. The jets are defined by at most two partons using the  $k_T$  algorithm with a separation  $\Delta R = 0.8$ , where  $\Delta R = \sqrt{(y_1 - y_2)^2 + (\phi_1 - \phi_2)^2}$ ,  $y_i = 1/2 \ln(E_i - p_{i,z})/(E_i + p_{i,z})$  being the rapidity and  $\phi_i$  the azimuthal angle of parton  $i$ . Moreover, the recombination is only performed if both partons satisfy  $|y_i| < 5$  (approximate detector bounds). We further assume for  $t\bar{t}b\bar{b}$  ( $t\bar{t}jj$ ) processes, that the jets are separated by  $\Delta R = 0.8$  (1.0) and have  $|y_{jet}| < 2.5$  (4.5). Their transverse momentum is required to be larger than 20 (50) GeV respectively. We consistently use the CTEQ6 set of parton distribution functions, i.e. we take CTEQ6L1 PDFs with a 1-loop running  $\alpha_s$  in LO and CTEQ6M PDFs with a 2-loop running  $\alpha_s$  at NLO.

We begin our presentation of the final results of our analysis with a discussion of the total cross section. At the central value of the scale,  $\mu_R = \mu_F = \mu_0 = m_t$ , we have obtained

$$\begin{aligned} \sigma_{pp \rightarrow t\bar{t}b\bar{b}+X}^{\text{LO}} &= 1489.2^{+1036.8(70\%)}_{-565.8(38\%)} \text{ fb}, & \sigma_{pp \rightarrow t\bar{t}b\bar{b}+X}^{\text{NLO}} &= 2636^{+862(33\%)}_{-703(27\%)} \text{ fb}, \\ \sigma_{pp \rightarrow t\bar{t}jj+X}^{\text{LO}} &= 120.17^{+87.14(72\%)}_{-46.64(39\%)} \text{ pb}, & \sigma_{pp \rightarrow t\bar{t}jj+X}^{\text{NLO}} &= 106.94^{+14.30(13\%)}_{-13.28(12\%)} \text{ pb}, \end{aligned}$$

where the error comes from varying the scale up and down by a factor 2. From the above result one can obtain  $K$  factors

$$K_{pp \rightarrow t\bar{t}b\bar{b}+X} = 1.77, \quad K_{pp \rightarrow t\bar{t}jj+X} = 0.89.$$

In case of  $pp \rightarrow t\bar{t}b\bar{b} + X$  corrections are large of the order of 77%. However, they can be reduced substantially, even down to -11%, either by applying additional cuts or by a better choice of

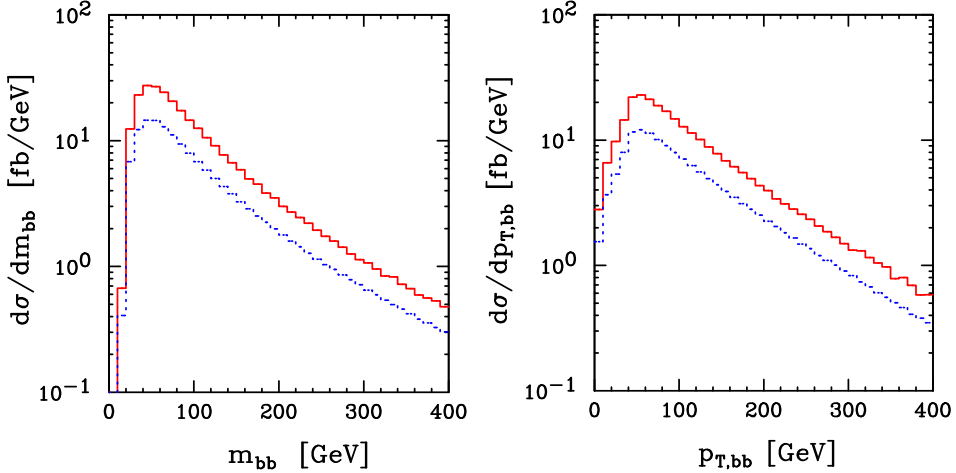


Figure 2: Distribution of the invariant mass  $m_{b\bar{b}}$  (left panel) and the distribution in the transverse momentum  $p_{T,b\bar{b}}$  (right panel) of the bottom-anti-bottom pair for  $pp \rightarrow t\bar{t}b\bar{b} + X$  at the LHC. The blue dotted curve corresponds to the LO whereas the red solid to the NLO one.

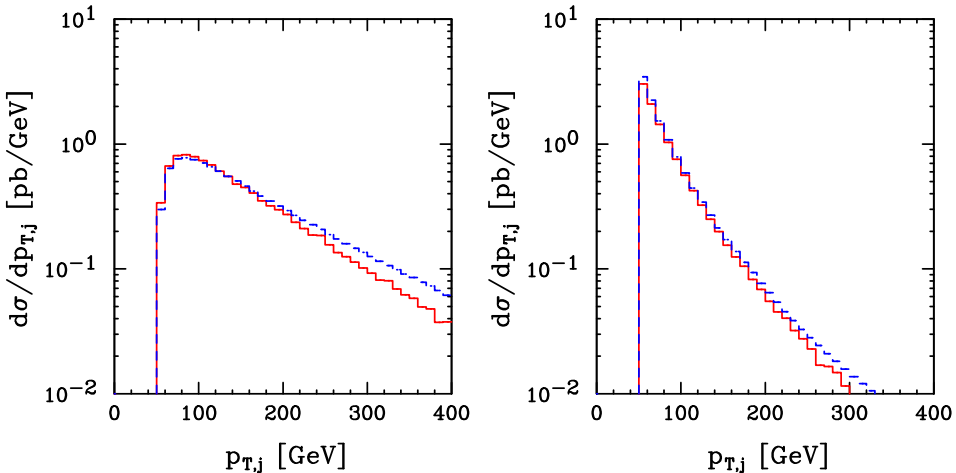


Figure 3: Distribution in the transverse momentum  $p_{T,j}$  of the 1st hardest jet (left panel) and the 2nd hardest jet (right panel) for  $pp \rightarrow t\bar{t}jj + X$  at the LHC. The blue dotted curve corresponds to the LO whereas the red solid to the NLO one.

factorization and renormalization scales as already suggested by Bredenstein et al.<sup>16</sup>. In case of  $pp \rightarrow t\bar{t}jj + X$  we have obtained negative corrections of the order of 11%. In both cases a dramatic reduction of the scale uncertainty is observed while going from LO to NLO. The scale dependence of the corrections for both processes is graphically presented in Fig. 1.

While the size of the corrections to the total cross section is certainly interesting, it is crucial to study the corrections to the distributions. In Fig. 2 the differential distributions for two observables, namely the invariant mass and transverse momentum of the two- $b$ -jet system are depicted for the  $pp \rightarrow t\bar{t}b\bar{b} + X$  process. Clearly, the distributions show the same large corrections, which turn out to be relatively constant contrary to the quark induced case<sup>17</sup>. In Fig. 3 the transverse momentum distributions of the hardest and second hardest jet are shown for the  $pp \rightarrow t\bar{t}jj + X$  process. Distributions demonstrate tiny corrections up to at least 200 GeV, which means that the size of the corrections to the cross section is transmitted to the distributions. On the other hand, strongly altered shapes are visible at high  $p_T$  especially in case of the first hardest jet. Let us underline here, that corrections to the high  $p_T$  region can

only be correctly described by higher order calculations and are not altered by soft-collinear emissions simulated by parton showers.

## Conclusions

A brief summary of the calculations of NLO QCD corrections to the background processes  $pp \rightarrow t\bar{t}b\bar{b} + X$  and  $pp \rightarrow t\bar{t}jj + X$  at the LHC has been presented. They have been calculated with the help of the HELAC-NLO system.

The QCD corrections to the integrated cross section for the irreducible background are found to be very large, changing the LO results by about 77%. The distributions show the same large corrections which are relatively constant. The residual scale uncertainties of the NLO predictions are at the 33% level. On the other hand, the corrections to the reducible background with respect to LO are negative and small, reaching 11%. The error obtained by scale variation is of the same order. The size of the corrections to the cross section is transmitted to the distributions at least for the low  $p_T$  region. However, the shapes change appreciably at high  $p_T$ .

## Acknowledgments

I would like to thank the organizers of Rencontres de Moriond for the kind invitation and the very pleasant atmosphere during the conference. The work presented here was funded by the Initiative and Networking Fund of the Helmholtz Association, contract HA-101 (“Physics at the Terascale”) and by the RTN European Programme MRTN-CT-2006-035505 HEPTOOLS - Tools and Precision Calculations for Physics Discoveries at Colliders.

## References

1. G. L. Bayatian *et al.* [CMS Collaboration], *J. Phys. G* **34**, 995 (2007).
2. G. Aad *et al.* [The ATLAS Collaboration], arXiv:0901.0512 [hep-ex].
3. A. Bredenstein, A. Denner, S. Dittmaier and S. Pozzorini, *Phys. Rev. Lett.* **103**, 012002 (2009).
4. G. Bevilacqua, M. Czakon, C. G. Papadopoulos, R. Pittau and M. Worek, *J. High Energy Phys.* **0909**, 109 (2009).
5. G. Bevilacqua, M. Czakon, C. G. Papadopoulos and M. Worek, arXiv:1002.4009 [hep-ph].
6. A. Kanaki and C. G. Papadopoulos, *Comput. Phys. Commun.* **132**, 306 (2000).
7. C. G. Papadopoulos, *Comput. Phys. Commun.* **137**, 247 (2001).
8. A. Cafarella, C. G. Papadopoulos and M. Worek, *Comput. Phys. Commun.* **180**, 1941 (2009).
9. G. Ossola, C. G. Papadopoulos and R. Pittau, *J. High Energy Phys.* **0803**, 042 (2008).
10. G. Ossola, C. G. Papadopoulos and R. Pittau, *Nucl. Phys. B* **763**, 147 (2007).
11. G. Ossola, C. G. Papadopoulos and R. Pittau, *J. High Energy Phys.* **0805**, 004 (2008).
12. P. Draggiotis, M. V. Garzelli, C. G. Papadopoulos and R. Pittau, *J. High Energy Phys.* **0904**, 072 (2009).
13. A. van Hameren, C. G. Papadopoulos and R. Pittau, *J. High Energy Phys.* **0909**, 106 (2009).
14. M. Czakon, C. G. Papadopoulos and M. Worek, *J. High Energy Phys.* **0908**, 085 (2009).
15. S. Catani, S. Dittmaier, M. H. Seymour and Z. Trocsanyi, *Nucl. Phys. B* **627**, 189 (2002).
16. A. Bredenstein, A. Denner, S. Dittmaier and S. Pozzorini, arXiv:1001.4006 [hep-ph].
17. A. Bredenstein, A. Denner, S. Dittmaier and S. Pozzorini, *J. High Energy Phys.* **0808**, 108 (2008).